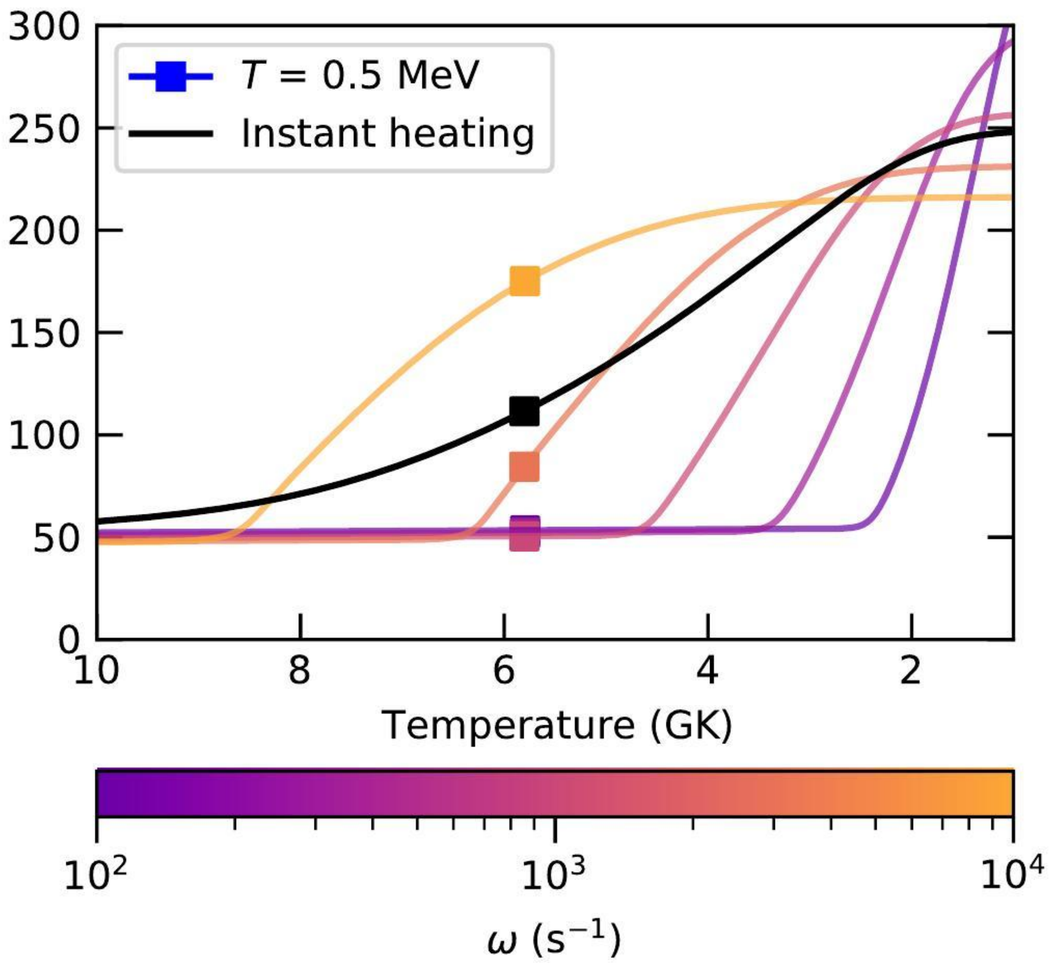

Figure 5. Early entropy profiles for a 1.5 $M_\odot$ neutron star with $L_\nu = 3 \times 10^{52}$ erg s^{-1} and $L_w = 10^{-3} L_\nu$ with varied wave frequencies. For higher frequencies, the shock heating begins to increase the entropy in the wind earlier and has a larger impact where seed nuclei are formed. The impact of the shock prescription is illustrated by the black line, which shows the evolution of the entropy if the waves (with $\omega = 2 \times 10^3$ rad s^{-1}) shock immediately instead of when equation 13 dictates.

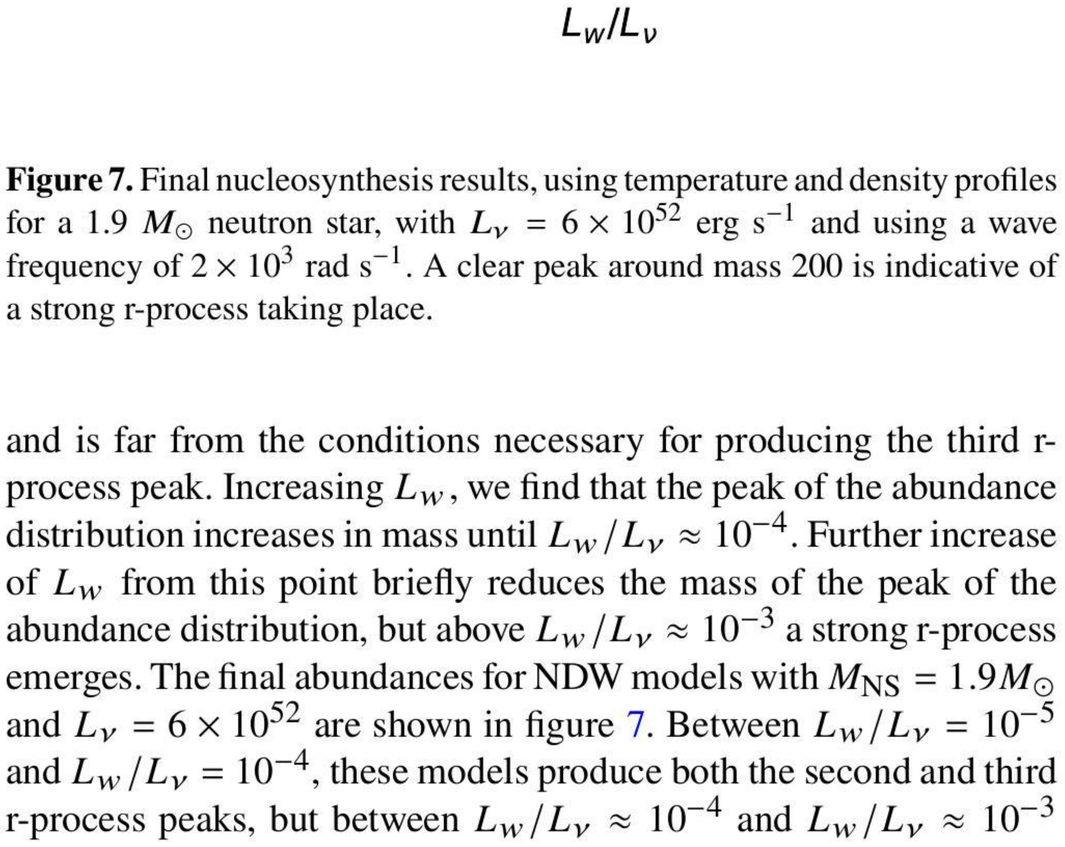

Figure 7. Final nucleosynthesis results, using temperature and density profiles for a 1.9 $M_\odot$ neutron star, with $L_\nu = 6 \times 10^{52}$ erg s^{-1} and using a wave frequency of 2×10^3 rad s^{-1}. A clear peak around mass 200 is indicative of a strong r-process taking place.

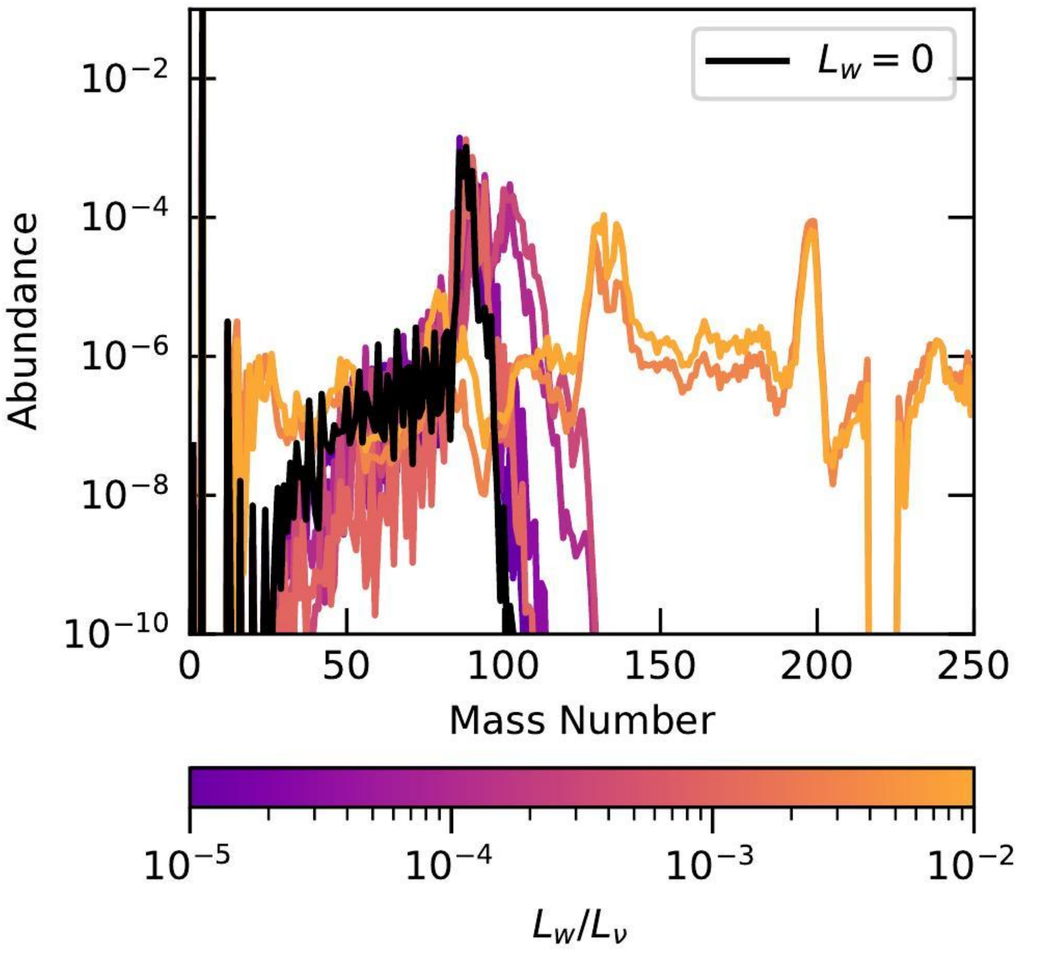

Figure 6. Final nucleosynthesis results, using temperature and density profiles for a 1.5 $M_\odot$ neutron star, with $L_\nu = 3 \times 10^{52}$ erg s^{-1} and using a wave frequency of 2×10^3 rad s^{-1}. A clear peak around mass 200 is indicative of a strong r-process taking place.

and is far from the conditions necessary for producing the third r-process peak. Increasing L_w, we find that the peak of the abundance distribution increases in mass until $L_w/L_\nu \approx 10^{-4}$. Further increase of L_w from this point briefly reduces the mass of the peak of the abundance distribution, but above $L_w/L_\nu \approx 10^{-3}$ a strong r-process emerges. The final abundances for NDW models with $M_{\rm NS} = 1.9 M_\odot$ and $L_\nu = 6 \times 10^{52}$ are shown in figure 7. Between $L_w/L_\nu = 10^{-5}$ and $L_w/L_\nu = 10^{-4}$, these models produce both the second and third r-process peaks, but between $L_w/L_\nu \approx 10^{-4}$ and $L_w/L_\nu \approx 10^{-3}$ production of the third peak is again cutoff and the peak of the abundance distribution is pushed down to lower mass. As L_w/L_ν is increased above 10^{-3}, a strong r-process re-emerges.

For both sets of parameters, we find the interesting behavior that r-process nucleosynthesis is inhibited for L_w/L_ν in the approximate range of 10^{-4} - 10^{-3}. This turnover in the maximum mass number is due to the competition between the decreasing dynamical timescale (τ_d) with L_w, which inhibits seed formation, and the decreasing entropy (s) with L_w, which facilitates seed production by increasing the density at which alpha recombination occurs (Hoffman et al. 1997). Figure 8 illustrates the correlation between the quantity $s^3/Y_e^3\tau_d$ and the total abundance above mass 150. Despite entropy no longer being constant during seed formation, we do observe a fairly strong correlation between r-process strength and this quantity. We find that as the wave luminosity is increased, τ_d decreases slightly faster than the entropy, but eventually asymptotes to a minimum value of a few times 10^{-4} s. The entropy continues to steadily decrease, which creates the trough in $s^3/Y_e^3\tau_d$ as a function of L_w and gives rise to the window of inhibited r-processing we observe around $L_w/L_\nu = 10^{-3}$. At higher L_w, shock heating begins prior to alpha recombination, drastically increasing the entropy. This, coupled with the reduced electron fraction at high L_w, reinvigorates a strong r-process.

Second, we consider the impact of varying ω on gravito-acoustic NDW nucleosynthesis. As was noted above, increasing ω results in an earlier activation of shock heating. In figure 9, we show the